Journal of Computer Science and Electrical Engineering
ISSN: 2663-1946
DOI: https://doi.org/10.61784/jcsee3068

SELECTION STRATEGY FOR FULL-SPECTRUM VERSUS LOCAL-SPECTRUM ENERGY DETECTION UNDER CONSTANT FALSE ALARM RATE CONDITIONS

YuXin Cheng
School of Intelligent Equipment, Shandong University of Science and Technology, Taian 271000, Shandong, China.
Corresponding Email: 15166744447@163.com

Abstract: In information science and electrical engineering, energy detection is a foundational tool for dynamic spectrum access and environmental awareness, playing a critical role in modern wireless communication systems. While Local Spectrum Energy Detection (LSED) is commonly regarded as superior to Full Spectrum Energy Detection (FSED), its performance advantage is not guaranteed across all real-world conditions. In this study, we derive closed-form expressions for the false alarm and detection probabilities of both FSED and LSED under the constant false alarm rate (CFAR) criterion. To address varying signal distributions, we develop an analytical framework based on the SNR ratio and categorize the frequency band selection problem into two typical cases: complete and partial capture of signal energy. Monte Carlo simulations validate our theoretical findings and reveal the specific conditions under which LSED provides measurable benefits over FSED, such as in narrowband signal environments or when prior knowledge of the signal's spectral characteristics is available. Furthermore, we propose a novel frequency-band energy ratio metric, which quantifies the relative energy distribution across different bands, enabling adaptive and resource-efficient detection method selection in complex electromagnetic environments. This metric facilitates intelligent switching between FSED and LSED based on real-time spectrum conditions. This work offers theoretical insights and practical guidance for signal detection, spectrum sensing, and data-driven decision-making in electronic communication and IoT-enabled systems, contributing to more efficient spectrum utilization and improved reliability in next-generation wireless networks.
Keywords: Constant false alarm rate; Energy detection; Full spectrum; Local spectrum

1 INTRODUCTION

Energy detection technology is widely used in the field of cognitive radio due to its reliable performance and relatively simple implementation [1]. Energy detection can be divided into time-domain energy detection (TDED) and frequency-domain energy detection (FDED) [2-4]. TDED uses the sum of the squares of the time-domain amplitudes of the sensing signals as the test statistic, while FDED uses the accumulation of the power spectrum within the sensing bandwidth as the test statistic.

FDED can be classified into two categories based on the spectrum of interest. When the focus is on the entire power spectrum, and the sum of the power spectra of all spectral lines within the detection length is used as the test statistic, it is referred to as Full Spectrum Energy Detection (FSED) [5]. In contrast, if only a specific sub-band is considered, and the sum of the power spectra of spectral lines from the start to the end of the band is used as the test statistic, it is referred to as Local Spectrum Energy Detection (LSED) [6].

LSED is widely favored in signal detection applications. Some authors proposed a two-level fuzzy logic-based detection system for local spectrum sensing [7]. A strategy using a simple recursive estimator was introduced to enhance the reliability of local spectrum sensing in cognitive radio networks [8]. A spectrum sensing technology designed for reliable signal detection in very low SNR environments was explored [9]. A local spectrum sensing model was established in cognitive wireless sensor networks to improve achievable throughput and enhance robustness across different environments [10].

It is generally believed that Local Spectrum Energy Detection (LSED) can achieve better detection performance than Full Spectrum Energy Detection (FSED) by focusing on frequency bands with more concentrated signal energy; however, this assumption has not been fully validated. LSED targets a selected sub-band, where the number of spectral lines and the signal-to-noise ratio (SNR) vary across different frequency regions, resulting in varying detection performance. This paper investigates the SNR relationship between LSED and FSED, with particular emphasis on how the symmetry of signal energy distribution influences detection efficiency. A comparative analysis of the detection performance of LSED and FSED is conducted, and the Excellent Energy Ratio (EER) is introduced based on the derived SNR relationship. The EER serves as a robust criterion for selecting LSED and offers practical guidance for energy detection method selection in real-world applications.

This paper analyzes the detection performance of both methods under the Constant False Alarm Rate (CFAR) condition [11], where the false alarm probability remains constant, and the detection performance is determined by their respective detection probabilities. Recently, CFAR technology has made significant breakthroughs. A deep learning framework was developed to train neural networks that approximate CFAR [12]. A novel constant false positive detection method based on the Gaussian Mixture Model (GMM), using Gabor wavelets to determine the number of

GMM components, was proposed [13]. Bayesian optimization was integrated into the Maximum Constant False Alarm Rate (GO-CFAR) for the prediction of maximum frequency hopping (FH) [14]. Future research will explore further advancements in CFAR technologies.

Additionally, we conducted Monte Carlo simulation experiments, using sinusoidal signals to simulate narrowband signals and Ricker wavelets to simulate broadband signals [15-16]. We then compared the actual and theoretical probabilities. The results confirm that the theoretical analysis is correct.

The remainder of this paper is organized as follows: Section 2 analyzes the mathematical model of signal detection in the frequency domain and derives the formulas for the detection probabilities of FSED and LSED. Section 3 evaluates the detection performance of both methods under various conditions and outlines the method selection strategy. Section 4 presents simulation experiments using narrowband and broadband signals to validate the theoretical derivation in Section 3. Section 5 discusses the relevant aspects of the research process. Finally, Section 6 concludes the paper.

2 THEORETICAL MODEL

The frequency-domain energy detection model is the core component of energy detection technology, primarily used to analyze the energy distribution of signals in the frequency domain. This model can be divided into two methods: Full Spectrum Energy Detection (FSED) and Local Spectrum Energy Detection (LSED). FSED focuses on the entire spectrum, determining the presence of a signal by summing the power spectra of all frequency components. On the other hand, LSED concentrates on a specific frequency band of interest, analyzing only the frequency components within a certain range. This approach is equivalent to applying a band-pass filter to the signal before performing energy detection. In the signal detection process, the received signal can be considered as a binary hypothesis problem, where the signal either exists or does not exist. To implement frequency-domain energy detection, the received signal needs to be transformed from the time domain to the frequency domain using a discrete Fourier transform. After the transformation, the spectrum is divided into positive and negative frequency parts. However, to simplify the analysis, only the positive frequency part of the spectrum is typically considered. By calculating the power spectrum using the periodogram method, the energy distribution at each frequency point can be obtained, providing a basis for further detection.

2.1 Full Spectrum Energy Detection Model

FSED takes the sum of all spectral lines in the power spectrum as the test statistic, that is:

$$T_{FD} = \sum_{k=0}^{N/2-1} P(k) \tag{1}$$

If the signal-to-noise ratio is $\gamma = \frac{2}{N^2\sigma_z^2} \sum_{k=0}^{N/2-1} \left(X_R^2(k) + X_I^2(k) \right)$, then, for sufficiently large detection length N, the central limit theorem indicates that the N independent random variables follow a Gaussian distribution:

$$T_{FD} \sim \begin{cases} \mathcal{N}\left(N\sigma_z^2/2, N\sigma_z^4/2 \right) & H_0 \\ \mathcal{N}\left((1+\gamma)N\sigma_z^2/2, (1+2\gamma)N\sigma_z^4/2 \right) & H_1 \end{cases} \tag{2}$$

Let the decision threshold be η_{FD} . According to the Neyman-Pearson criterion, the following expression can be derived:

$$P_f = \Pr\left(T_{FD} \geq \eta_{FD} \mid H_0 \right) = Q\left(\frac{\eta_{FD} - \frac{N}{2}\sigma_z^2}{\sqrt{\frac{N}{2}}\sigma_z^2} \right), \tag{3}$$

$$\eta_{FD} = \left(Q^{-1}(P_f)\sqrt{N/2} + N/2 \right)\sigma_z^2, \tag{4}$$

$$P_d = \Pr\left(T_{FD} > \eta_{FD} \mid H_1 \right) = Q\left(\frac{Q^{-1}(P_f) - \gamma\sqrt{\frac{N}{2}}}{\sqrt{1+2\gamma}} \right), \tag{5}$$

where P_f is the false alarm probability, P_d is the detection probability, and Q is the right-tail probability function of the standard normal distribution.

2.2 Local Spectrum Energy Detection Model

If the frequency band of interest consists of d spectral lines P(i), P(i+1) …… P(i+d-1), then the detection statistic can be defined as:

$$T_{LS}(i,d)=\sum_{k=i}^{i+d-1}P(k) \tag{6}$$

where i represents the number of the spectral line at the beginning of the frequency band, and d represents the number of spectral lines. In the simulation experiment, if the selected frequency band range is 20-50Hz, i is 20 and d is 30. Let the local spectral SNR of this band be $\gamma_i'=\frac{1}{dN\sigma_z^2}\sum_{k=i}^{i+d-1}\left(X_R^2(k)+X_I^2(k)\right)$, which reflects the ratio of effective signal to noise energy in the band of interest. LSED can be represented by an approximate Gaussian distribution. According to the central limit theorem, we can get:

$$T_{LS}\sim\begin{cases}\mathcal{N}\left(d\sigma_z^2,d\sigma_z^4\right) & H_0\\ \mathcal{N}\left((1+\gamma')d\sigma_z^2,(1+2\gamma')d\sigma_z^4\right) & H_1\end{cases} \tag{7}$$

Set the detection threshold as η_{LS}, then:

$$P_f=\Pr\left(T_{LS}\geq\eta_{LS}\right)=Q\left(\frac{\eta_{LS}-d\sigma_z^2}{\sqrt{d}\sigma_z^2}\right), \tag{8}$$

$$\eta_{LS}=\sqrt{d}\sigma_z^2Q^{-1}(P_f)+d\sigma_z^2\ , \tag{9}$$

$$P_d=\Pr\left(T_{LS}>\eta_{LS}\mid H_1\right)=Q\left(\frac{Q^{-1}(P_f)-\gamma'\sqrt{d}}{\sqrt{1+2\gamma'}}\right). \tag{10}$$

3 SELECTION STRATEGY ANALYSIS

Through the derivation above, under the Constant False Alarm Rate (CFAR) condition, the detection performance of both methods depends on their respective detection rates. The detection rates of both methods are described using Q functions, so the performance comparison essentially boils down to comparing the Q function values under identical conditions. Since the Q function is a monotonically decreasing function, the larger the argument, the smaller its value. Let the inverse of the Q function be denoted as $A=Q^{-1}(P_f)$, where A is also a decreasing function. Since a high false alarm rate is generally considered meaningless, the range of P_f is constrained to (0, 0.5], which implies that A > 0.

We define the function $f(A,N,\gamma)$ as follows:

$$f(A,N,\gamma)=\frac{A-\gamma\sqrt{N/2}}{\sqrt{1+2\gamma}}\ . \tag{11}$$

Let the function $f(A,2d,\gamma')$ be defined as follows:

$$f(A,2d,\gamma')=\frac{A-\gamma'\sqrt{d}}{\sqrt{1+2\gamma'}}\ . \tag{12}$$

The two functions are the independent variable functions in equations (9) and (14). The smaller their values, the greater the corresponding detection probability. Moreover, $1\leq d<N/2$, with only the spectrum of the positive frequency component being considered.

Let the ratio of the signal-to-noise ratio of the two methods be a, that is:

$$\gamma'=a\gamma \tag{13}$$

Analyze separately the cases where the frequency band contains a portion of the signal energy and the cases where the frequency band contains the entire signal energy.

3.1 The Frequency Band Contains a Portion of the Signal Energy

3.1.1 The SNR of LSED is lower than that of FSED

In this case, a < 1. First, let's analyze the monotonicity of the function $f(A,N,\gamma)$. The partial derivative of $f(A,N,\gamma)$ with respect to N is:

$$\frac{\partial f(A,N,\gamma)}{\partial N}=\frac{-\gamma}{2\sqrt{2}\sqrt{1+2\gamma}\sqrt{N}}<0\ . \tag{14}$$

When γ and A are constant, $f(A,N,\gamma)$ decreases as N increases. The partial derivative of $f(A,N,\gamma)$ with respect to γ is given by:

$$\frac{\partial f(A,N,\gamma)}{\partial \gamma}=\frac{-A-\sqrt{N/2}\ -\gamma\sqrt{N/2}}{(1+2\gamma)\sqrt{1+2\gamma}}<0\ . \tag{15}$$

When N and A are constant, $f(A,N,\gamma)$ decreases as γ increases.

Based on the analysis above, since d < N/2, we have $f(A,N,\gamma)<f(A,2d,\gamma)$. Furthermore, since $\gamma'<\gamma$, it follows that $f(A,2d,\gamma)<f(A,2d,\gamma')$. Therefore, $f(A,N,\gamma)<f(A,2d,\gamma')$.

Given that the Q function is a decreasing function, the detection probability of FSED is higher, making it preferable to choose FSED.

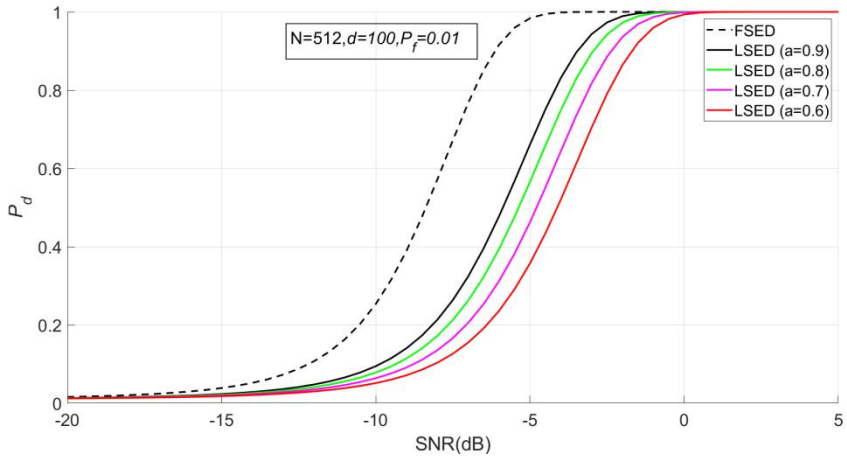

Figure 1 Graph of the Detection Probabilities for FSED and LSED When a < 1

As shown in Figure 1, when a < 1, the P_d of FSED is always higher than that of LSED.

3.1.2 The SNR of LSED is greater than or equal to FSED

In this case, $a \geq 1$. Substituting equation (13) into equation (12) yields:

$$f(A,2d,\gamma')=\frac{A-a\gamma\sqrt{d}}{\sqrt{1+2a\gamma}}\ . \tag{16}$$

The partial derivative of $f(A,2d,\gamma')$ with respect to a is:

$$\frac{\partial f(A,2d,\gamma')}{\partial a}=\frac{-\gamma'\left(\sqrt{d}+2A\right)}{(1+2a\gamma')\sqrt{1+2a\gamma'}}<0. \tag{17}$$

Therefore, $f(A,2d,\gamma')$ is a decreasing function of a. The relationship between $f(A,N,\gamma)$ and $f(A,2d,\gamma')$ is shown in the figure below:

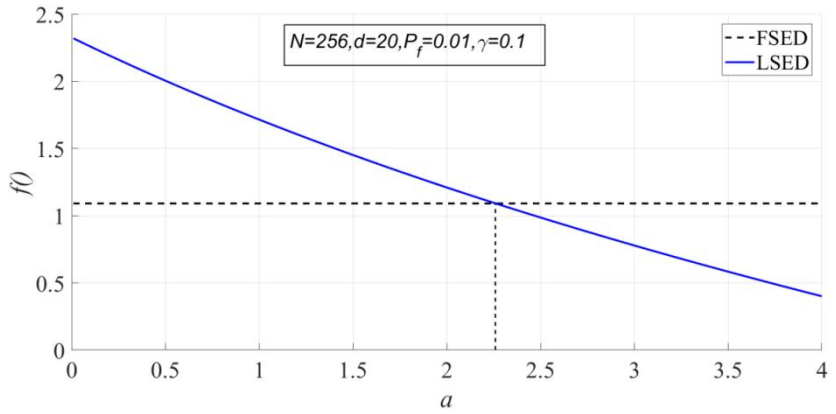

Figure 2 Graph of the Independent Variable Functions for FSED and LSED When $a \geq 1$

In Figure 2, when γ, N, and P_f are fixed, the value of $f(A,N,\gamma)$ remains constant and does not vary with a, resulting in a horizontal line. Meanwhile, $f(A,2d,\gamma')$ decreases as a increases. The two functions intersect at a specific point. To the left of this intersection, the detection performance of LSED is worse than that of FSED, while to the right, LSED outperforms FSED. The intersection point can be determined by solving equation (18):

$$\frac{A-a\gamma\sqrt{d}}{\sqrt{1+2a\gamma}}=\frac{A-\gamma\sqrt{N/2}}{\sqrt{1+2\gamma}}. \tag{18}$$

Let $T=\frac{A-\gamma\sqrt{N/2}}{\sqrt{1+2\gamma}}$, then equation (18) can be simplified as follows:

$$\gamma^2 d a^2-(2A\gamma\sqrt{d}+2\gamma T^2)a+A^2-T^2=0 \tag{19}$$

The discriminant of the root of the unary quadratic equation with respect to a is:

$$\Delta=4\left[T^2+2A\sqrt{d}+d\right]\gamma^2T^2\geq 0 \tag{20}$$

If $\Delta=0$, equation (18) has only one solution, which is T = 0, and $\gamma=\sqrt{2/NA}$.

At this point, $a=\sqrt{\frac{N}{2d}}$. That is, when $a<\sqrt{\frac{N}{2d}}$, LSED performs worse than FSED; when $a>\sqrt{\frac{N}{2d}}$, LSED outperforms FSED.

If $\Delta>0$, two solutions of equation (19) can be obtained according to the quadratic formula, respectively:

$$a_1=\frac{A\sqrt{d}+T^2+|T|\sqrt{T^2+2A\sqrt{d}+d}}{\gamma d},\ a_2=\frac{A\sqrt{d}+T^2-|T|\sqrt{T^2+2A\sqrt{d}+d}}{\gamma d} \tag{21}$$

Obviously, $a_1>a_2$. From Figure 2, it can be seen that there is only one intersection point between the two curves, so there cannot be two solutions. Therefore, only one solution is valid. The following is an analysis of the cases where T > 0 and T < 0, respectively.

3.1.2.1 When T > 0, that is, $\gamma<\sqrt{2/N}A$

In this case, both sides of equation (18) must be greater than 0, i.e., $A-a\gamma\sqrt{d}>0$ and $a<\frac{A}{\gamma\sqrt{d}}$. Substituting a_1 into equation (18), we obtain:

$$a_1-\frac{A}{\gamma\sqrt{d}}=\frac{T^2+|T|\sqrt{T^2+2A\sqrt{d}+d}}{\gamma d}>0 \tag{22}$$

That is, $a_1>\frac{A}{\gamma\sqrt{d}}$, and it is evident that a_1 does not meet the requirements. Substituting a_2 into equation (18) to obtain:

$$a_2-\frac{A}{\gamma\sqrt{d}}=\frac{T^2-|T|\sqrt{T^2+2A\sqrt{d}+d}}{\gamma d}<0 \tag{23}$$

That is, $a_2 < \frac{A}{\gamma\sqrt{d}}$, and it is evident that a_2 meets the requirements. Therefore, when $\gamma < \sqrt{2/NA}$, if $a < a_2$, then $f(A,N,\gamma) < f(A,2d,\gamma')$, and selecting FSED is preferable. If $a > a_2$, then $f(A,N,\gamma) > f(A,2d,\gamma')$, and selecting LSED is preferable.

Let N = 256, d = 20, P_f = 0.01, and γ = 0.1. In this case, $\sqrt{2/NA}$ = 0.2056, and $\gamma < \sqrt{2/NA}$. The intersection occurs at a_2 = 2.2626.

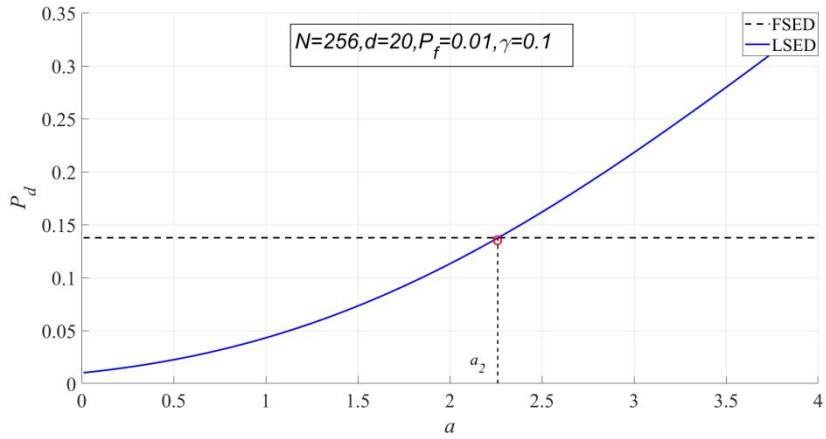

Figure 3 Graph of the Detection Probabilities for FSED and LSED When $\gamma < \sqrt{2/NA}$

It can be seen from Figure 3 that when $a > a_2$, the detection probability of LSED is higher than that of FSED. When $a < a_2$, the detection probability of LSED is lower than that of FSED.

3.1.2.2 When T < 0, that is, $\gamma > \sqrt{2/NA}$

At this point, $A - a\gamma\sqrt{d} < 0$ and $a > \frac{A}{\gamma\sqrt{d}}$. As previously deduced, $a_1 - \frac{A}{\gamma\sqrt{d}} > 0$ and $a_2 - \frac{A}{\gamma\sqrt{d}} < 0$. It is evident that a_1 meets the requirements, while a_2 does not. Therefore, when $\gamma > \sqrt{2/NA}$, if $a < a_1$, $f(A,N,\gamma) < f(A,2d,\gamma')$, selecting FSED is preferable; if $a > a_1$, $f(A,N,\gamma) > f(A,2d,\gamma')$, selecting LSED is preferable.

Let N = 256, d = 20, P_f = 0.01, and γ = 0.3. In this case, $\sqrt{2/NA}$ = 0.2056, and $\gamma > \sqrt{2/NA}$. The intersection occurs at a_1 = 2.7593.

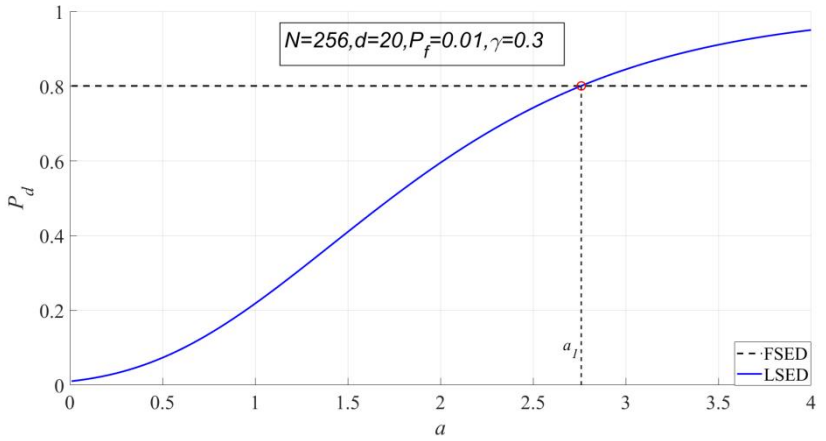

Figure 4 Graph of the Detection Probabilities for FSED and LSED When $\gamma > \sqrt{2/NA}$

It can be observed from Figure 4 that when $a > a_1$, the detection probability of LSED is higher than that of FSED. Conversely, when $a < a_1$, the detection probability of LSED is lower than that of FSED.

Based on the above analysis, the selection strategy for LSED and FSED when $a \geq 1$ is illustrated in the figure 5 below:

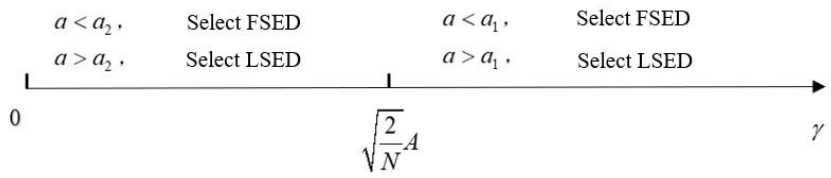

Figure 5 Selection Strategy for LSED and FSED When $a \geq 1$

3.2 The Frequency Band Contains All of the Signal Energy

Let the proportion of the energy contained in the selected frequency band to the total energy of the signal be defined as the frequency band energy ratio (ER), i.e.,

$$ER = \frac{\sum_{k=i}^{i+d-1}\left(X_R^2(k)+X_I^2(k)\right)}{\sum_{k=0}^{N/2-1}\left(X_R^2(k)+X_I^2(k)\right)} \tag{24}$$

The ratio of the signal-to-noise ratio \(a \) for the two methods is then given by:

$$a = \frac{\gamma'}{\gamma} = \frac{N}{2d}\frac{\sum_{k=i}^{i+d-1}\left(X_R^2(k)+X_I^2(k)\right)}{\sum_{k=0}^{N/2-1}\left(X_R^2(k)+X_I^2(k)\right)} \tag{25}$$

If ER = 1, it indicates that the entire spectral energy is concentrated in the frequency band of interest. In this case, $a = \frac{N}{2d}$, that is:

$$\gamma' = \frac{N}{2d}\gamma. \tag{26}$$

Then, equation (12) becomes:

$$f(A,2d,\gamma') = \frac{A-\frac{N}{2\sqrt{d}}\gamma}{\sqrt{1+\frac{N}{d}\gamma}} \tag{27}$$

Since $d < \frac{N}{2}$, it follows that $\frac{A-\sqrt{\frac{N}{2}}\gamma}{\sqrt{1+2\gamma}} > \frac{A-\frac{N}{2\sqrt{d}}\gamma}{\sqrt{1+\frac{N}{d}\gamma}}$. Therefore, $f(A,N,\gamma) > f(A,2d,\gamma')$. Under these conditions, the detection probability of LSED consistently exceeds that of FSED, making LSED the preferred option. Let P_f = 0.01, N = 512, and consider d = 10, 80, and 200 for the respective cases.

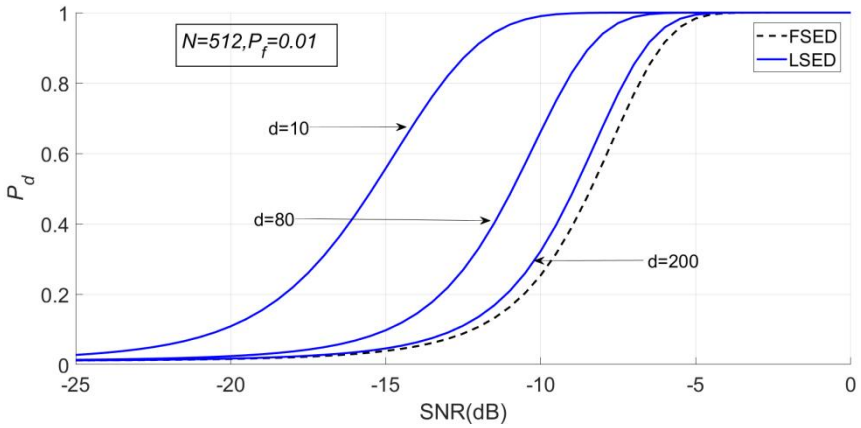

Figure 6 Graph of the Detection Probabilities for FSED and LSED When $\gamma' = \frac{N}{2d}\gamma$.

It can be observed from Figure 6 that as the parameter d increases, the performance of LSED becomes increasingly similar to that of FSED. This trend indicates that the difference in detection probability between the two methods narrows as d grows larger. However, despite this convergence, the detection probability of LSED remains consistently higher than that of FSED across all values of d. This superiority in performance demonstrates that LSED is better suited for scenarios where the frequency band encompasses the entire signal energy. Therefore, when the selected frequency band contains the complete energy of the signal, LSED emerges as the preferred option due to its superior detection capability.

4 SIMULATION EXPERIMENT

This section aims to validate the theoretical analysis results from Section 3 through Monte Carlo simulation experiments. These experiments are designed to test the performance of Full Spectrum Energy Detection (FSED) and Local Spectrum Energy Detection (LSED) under different conditions. To ensure comprehensive validation, two types of signals are used: sinusoidal signals to simulate narrowband signals and Ricker wavelets to simulate broadband signals. The experiments are conducted under controlled parameters, with the false alarm probability P_f set to 0.05, the detection length N fixed at 2048, and at least 10,000 independent Monte Carlo simulation tests performed to ensure statistical reliability.

4.1 The Frequency Band Contains All of the Signal Energy

In this experiment, sine signals are used to simulate narrowband signals, with Gaussian white noise added to generate the experimental data. The sine signal is configured with an amplitude of 0.5, a frequency of 30 Hz, and a phase of 0. The sampling frequency is set to 1024 Hz, and the sampling duration is 2 seconds, resulting in a frequency resolution of 0.5 Hz. The detection length N is set to 2048, ensuring sufficient data points for accurate analysis. To simplify the analysis, the spectrum used in this experiment is a unilateral spectrum, meaning only the positive frequency components are considered. This setup ensures that the selected frequency band contains the entire energy of the narrowband signal, allowing for a clear comparison between FSED and LSED.
The detection probabilities of the two detection methods after simulations with different values of d are as follows:

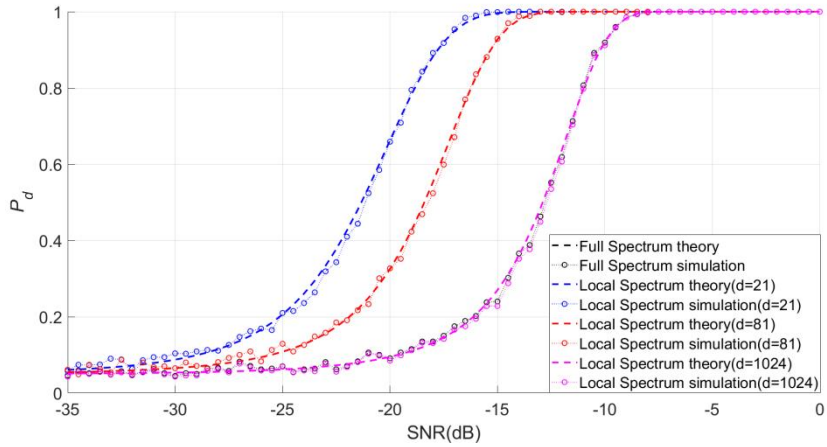

Figure 7 The Actual and Theoretical Detection Probabilities of Narrowband Signals Obtained from FSED and LSED Simulations under Different d

It can be observed from Figure 7 that the detection performance of LSED is always better than that of FSED. As d increases, LSED approaches FSED. When $\frac{N}{2d}=1$, i.e., $d=\frac{N}{2}$, the detection performance of the two methods becomes identical. As previously mentioned, since $d<\frac{N}{2}$, when the frequency band contains all the signal energy, LSED is always superior to FSED. This aligns with the theoretical analysis presented in Section 3.

4.2 The Frequency Band Contains a Portion of the Signal Energy

LSED is commonly used for microseismic monitoring, and the Ricker wavelet is frequently employed to simulate earthquake or microseismic signals in underground vibration simulation experiments. Therefore, the Ricker wavelet is chosen to simulate broadband signals in this study. The Ricker wavelet is particularly suitable for this purpose because it closely resembles the characteristics of real seismic signals, making it an ideal choice for testing the performance of energy detection methods in broadband scenarios. The time-domain expression of the Ricker wavelet is provided to describe its mathematical form, which helps in understanding its behavior in the frequency domain. This allows the selected frequency band to include only a portion of the signal energy, enabling the analysis of LSED's performance when the signal energy is not fully captured within the detection band.

$$s(t)=\left(1-2\pi^2 f_M^2 t^2\right)e^{-\pi^2 f_M^2 t^2} \quad , \tag{28}$$

Where t is the time and f_M is the peak frequency. The Fourier transform expression of the Ricker wavelet is given by:

$$S(f)=\frac{2f^2}{\sqrt{\pi}f_M^3}e^{-\frac{f^2}{f_M^3}} \quad . \tag{29}$$

The Ricker wavelet used in this experiment has a central frequency of 50 Hz, a duration of 2 seconds, a sampling frequency of 1024 Hz, a frequency resolution of 0.5 Hz, and a detection length N of 2048. In this case, the energy occupied by the local frequency band is easy to control. Let the frequency domain signal-to-noise ratio of FSED be γ , and the frequency domain signal-to-noise ratio of LSED be γ'. Let $\gamma'=a\cdot\gamma$, and analyze the detection rate.

Let N = 2048, P_f = 0.05, and $A=Q^{-1}(P_f)$. Then, $\sqrt{2/N}A=0.05$. When $\gamma=0.05$, the SNR is -13. The SNR refers to the time-domain signal-to-noise ratio of the global signal, which can be converted into noise variance to calculate the frequency-domain signal-to-noise ratio. SNR is proportional to γ .

The selected frequency band ranges are 65-90 Hz, 30-80 Hz, and 130-300 Hz. The corresponding values of d are 26, 51, and 171, and the values of a are 9.10, 4.52, and 1.51, respectively. The detection rates obtained through simulation are as follows:

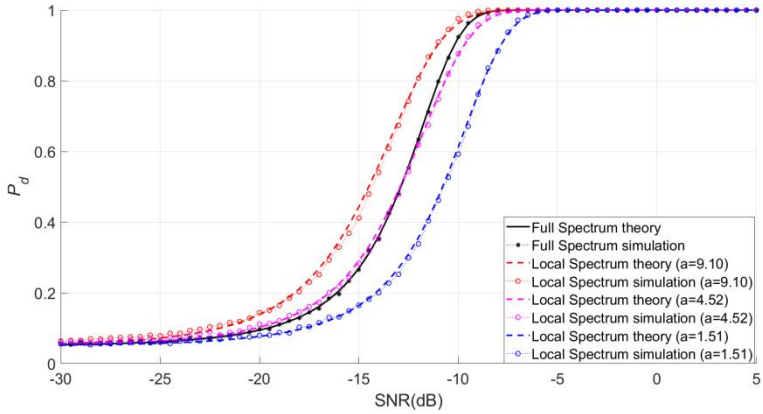

Figure 8 The Actual and Theoretical Detection Probabilities of Ricker Wavelet Obtained from FSED and LSED Simulations under Different a

Taking -13 dB as the dividing line, we use -15 dB and -11 dB as examples. When the SNR is -15 dB, γ = 0.03, the theoretical P_d of FSED is 0.2697, and the actual P_d is 0.2624. When the SNR is -11 dB, γ = 0.08, the theoretical P_d of FSED is 0.7976, and the actual P_d is 0.7942. The detection rates of a_1, a_2, and LSED in both cases are as follows:

Table 1 a_1 and P_d obtained in different frequency bands when $\gamma > \sqrt{2/NA}$

d	a	a1	Pd(theory)	Pd(simulation)
26	9.10	7.08	0.9042	0.9105
51	4.52	4.86	0.7579	0.7564
171	1.51	2.53	0.4716	0.4667

Table 2 a_1 and P_d obtained in different frequency bands when $\gamma < \sqrt{2/NA}$

d	a	a2	Pd(theory)	Pd(simulation)
26	9.10	5.72	0.4439	0.4228
51	4.52	4.21	0.2907	0.2783
171	1.51	2.38	0.1645	0.1610

From Table 1 and Table 2, when $\gamma > \sqrt{2/NA}$, in the first band where $a > a_1$, the detection rate of LSED is higher than that of FSED; in the second band where $a < a_1$, the detection rate of LSED is lower than that of FSED; in the third band where $a < a_1$, the detection rate of LSED remains lower than that of FSED.

When $\gamma < \sqrt{2/NA}$, in the first band where $a > a_2$, the detection rate of LSED is higher than that of FSED; in the second band where $a > a_2$, the detection rate of LSED is also higher than that of FSED; in the third band where $a < a_2$, the detection rate of LSED is lower than that of FSED. This is consistent with the theoretical analysis presented in Section 3.

4.3 Practical Application

To facilitate method selection in practical applications, we can establish clear guidelines by analyzing the frequency band energy ratio (ER). Specifically, when the energy ratio exceeds a certain threshold, referred to as the Excellent Energy Ratio (EER), it ensures that LSED outperforms FSED in terms of detection probability. This approach simplifies decision-making by allowing practitioners to focus on the energy concentration within the selected frequency band, ensuring optimal performance in real-world scenarios.

According to equations (24) and (25), the relationship between a and ER is as follows:

$$a = \frac{N}{2d} \cdot ER \tag{30}$$

It can be seen that a is proportional to ER. Therefore, we can calculate the maximum values of a_1 and a_2 within a certain range of signal-to-noise ratio, and determine the corresponding frequency band energy ratio, which we refer to as the EER. That is:

$$EER = \frac{2d}{N} \cdot \max(\max(a_1), \max(a_2)) \tag{31}$$

When ER is greater than EER, a must be greater than a_1 and a_2, and LSED must be better.

Let the false alarm probability P_f be 0.05, the detection length N be 2048, and the spectral line length d be 100. In Figure 8, when SNR > -5 dB, the detection rate is approximately 1, so only the case where SNR is in the range of -30 to -5 dB is analyzed below. In this interval, the maximum value of a_2 is 3.19, and the maximum value of a_1 is 4.67, with corresponding energy ratios of 31.15% and 45.61%. That is, when the frequency band energy ratio exceeds 45.61%, selecting LSED is definitely better than FSED. Other cases corresponding to the selected frequency bands can also be analyzed using this method.

The frequency bands selected are 125-224Hz, 3-102Hz, and 90-189Hz, with d = 100. The corresponding frequency band energy ratios are 30.46%, 45.63%, and 67.51%, respectively. The simulation results are as follows:

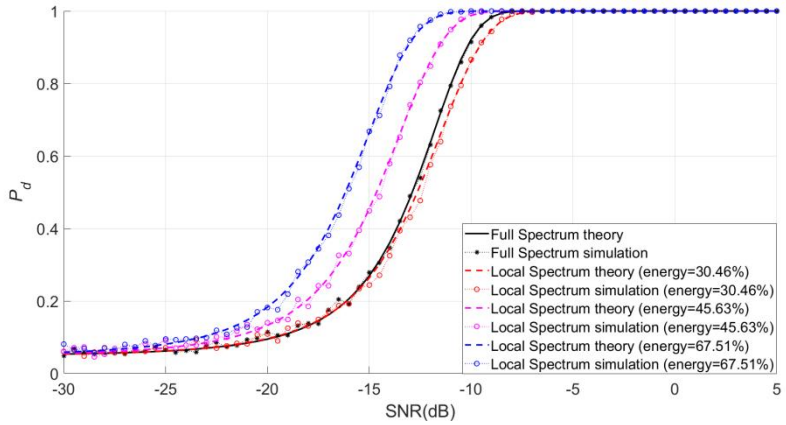

Figure 9 Detection Probabilities of LSED and FSED under Different Energy Ratios When d = 100

It can be seen from Figure 9 that when the energy ratio is 45.63% and 67.51%, i.e., ER > EER, the detection rate of LSED is higher than that of FSED. This indicates that LSED performs better when the frequency band captures a significant portion of the signal's energy. For example, at an SNR of -10 dB, LSED's detection probability is at least 7% higher than FSED, with the performance gain increasing as the energy ratio rises. When the energy ratio is 30.46%, i.e., ER < EER, the detection rate of LSED may be higher or lower than FSED, depending on the SNR conditions. Under low-SNR conditions, LSED outperforms FSED only if its SNR exceeds a specific threshold. In high-SNR scenarios, LSED becomes advantageous when the SNR ratio surpasses another threshold. This behavior aligns with the theoretical analysis, confirming that ER > EER ensures LSED's superiority.

5 DICUSSION

5.1 a_2 Can be Substituted in Practical Application

In the third part of the theoretical analysis, the calculation of a_2 is relatively complex. Through formula derivation, it is found that $a_2 < \sqrt{\frac{N}{2d}}$. Therefore, in practice, $\sqrt{\frac{N}{2d}}$ can be used as a substitute for a_2. Specifically, if $a > \sqrt{\frac{N}{2d}}$, the performance of LSED is superior to FSED; if $a < \sqrt{\frac{N}{2d}}$, the performance of FSED is better than LSED. Furthermore, when $\gamma < \sqrt{2/N}\,A$, indicating a low signal-to-noise ratio, it is more convenient to use $\sqrt{\frac{N}{2d}}$ under such conditions.

5.2 The Effect of N and d on EER

Next, the influence of detection length N and frequency band length d on the EER is analyzed. If the false alarm probability P_f is set to 0.05, the color chart of EER under different values of N and d is as follows:

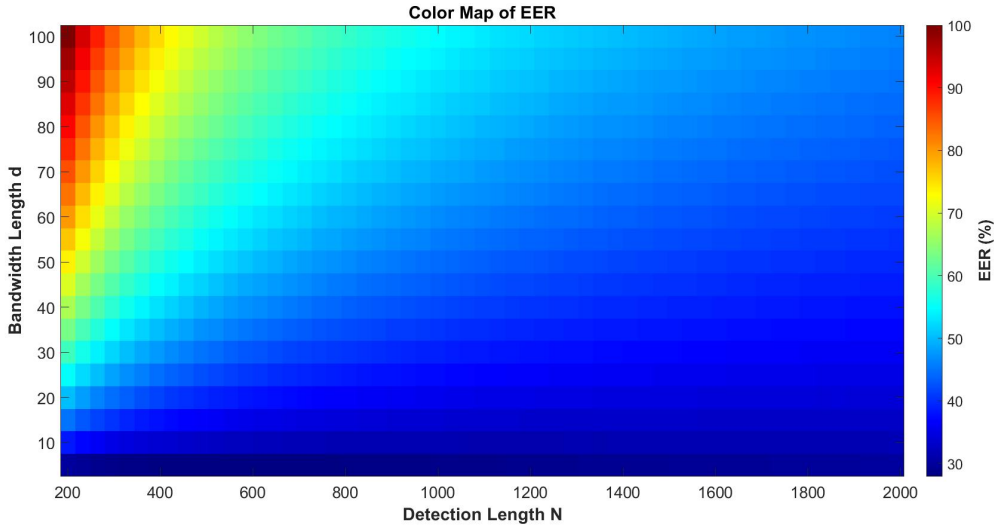

Figure 10 Color Map of EER under Different d and N

It can be observed from Figure 10 that the EER increases as d increases and decreases as N increases. Specifically, when d is large and N is small, the EER value is higher; conversely, when d is small and N is large, the EER value is lower.

5.3 a Indicates the Concentration Degree of the Signal Energy

In the simulation conducted in Section 4.3, the frequency band ranges are set to 125-224 Hz, 3-102 Hz, and 90-189 Hz, with the number of spectral lines, denoted as d, fixed at 100. The corresponding a values for these bands are 3.02, 4.79, and 6.81, respectively, while the energy proportions of the frequency bands are calculated to be 30.46%, 45.63%, and 67.51%. From these results, a clear trend emerges: for the same value of d, as the parameter a increases, the energy proportion of the frequency band also increases. This observation suggests that the frequency band is more concentrated in regions where the signal energy is higher. Consequently, a can be regarded as an indicator of the concentration of signal energy within the frequency band.

This relationship between a and the energy proportion highlights the utility of a as a metric for evaluating how effectively a chosen frequency band captures the dominant components of the signal's energy. When a is higher, it implies that the selected frequency band contains a larger share of the total signal energy, making it more suitable for applications where high detection performance is critical. Conversely, lower values of a indicate that the frequency band captures less of the signal's energy, potentially leading to suboptimal detection performance. This insight provides a practical guideline for selecting frequency bands in real-world applications, particularly when aiming to maximize the detection probability while minimizing resource usage. By leveraging a as an indicator, practitioners can make informed decisions about which frequency bands to prioritize based on their energy concentration characteristics.

6 CONCLUSIONS

This study establishes an optimal selection strategy between Local Spectrum Energy Detection (LSED) and Full Spectrum Energy Detection (FSED) by theoretically deriving the relationship between their signal-to-noise ratios (SNRs) and validating it through 10^4 Monte Carlo simulation experiments. The results indicate that, in full-band scenarios, the detection probability of LSED consistently exceeds that of FSED, and the performance gain is proportional to the bandwidth d, which represents the number of spectral lines analyzed within the frequency range (see Figure 6). Specifically, as the bandwidth d increases, the performance gap between LSED and FSED narrows, but LSED remains superior regardless of the specific value of d. In local-band scenarios, under low-SNR conditions, LSED outperforms FSED when its SNR exceeds that of FSED by a factor of a_2 . Under high-SNR conditions, however, LSED becomes advantageous only when the SNR ratio exceeds a higher threshold, denoted as a_1 , where $a_1 > a_2$.

The main contributions of this study are as follows: (1) A theoretical framework for detection method selection based on the SNR ratio a is established. This framework provides a systematic approach to determine the conditions under which LSED or FSED should be preferred, depending on the SNR ratio and the proportion of signal energy captured within the selected frequency band. (2) An efficient decision rule is proposed that relies solely on the frequency band energy ratio (ER), simplifying the selection process for practical applications. The results demonstrate that when the energy ratio exceeds the Excellent Energy Ratio (EER), the detection probability of LSED is at least 7% higher than that of FSED under an SNR of -10 dB. Furthermore, the performance gain increases proportionally with the energy

ratio, highlighting the importance of selecting frequency bands that capture a significant portion of the signal's energy (see Figure 9).

It is worth noting that the current analysis assumes additive white Gaussian noise, which is a common assumption in many signal processing applications. However, real-world scenarios often involve non-Gaussian noise environments, such as impulsive noise or cluttered backgrounds, which may affect the performance of both LSED and FSED. Future work will explore the applicability of the proposed framework under non-Gaussian noise environments and further evaluate its real-time performance. Additionally, the computational complexity and implementation feasibility of the proposed methods will be assessed to ensure their practical deployment in cognitive radio systems, seismic monitoring, and other relevant fields. These extensions aim to enhance the robustness and versatility of the energy detection techniques in diverse operational settings.

COMPETING INTERESTS

The authors have no relevant financial or non-financial interests to disclose.

REFERENCES

[1] Yucek T, Arslan H. A survey of pectrum sensing algorithms for cognitive radio applications. IEEE Communications Surveys & Tutorials 2009, 11, 116-130. DOI: https://doi.org/10.1109/SURV.2009.090109.

[2] Urkowitz H. Energy detection of unknown deterministic signals. Proceedings of the IEEE, 1967, 55, 523-531. DOI: https://doi.org/10.1109/PROC.1967.5573.

[3] Dikmese S, Ilyas Z, Sofotasios P C, et al. Sparse frequency domain spectrum sensing and sharing based on cyclic preffx autocorrelation. IEEE Journal on Selected Areas in Communications 2017, 35, 159-172. DOI: https://doi.org/10.1109/JSAC.2016.2633058.

[4] Hou C, Liu G, Tian Q, et al. Multisignal modulation classiffcation using sliding window detection and complex convolutional network in frequency domain. IEEE Internet of Things Journal, 2022, 9, 19438-19449. DOI: https://doi.org/10.1109/JIOT.2022.3167107.

[5] Li H, Hu Y, Wang S. A novel blind signal detector based on the entropy of the power spectrum subband energy ratio. Entropy, 2021, 23, 448. DOI: https://doi.org/10.3390/e23040448.

[6] Li H, Hu Y, Wang S. Signal detection based on power-spectrum sub-band energy ratio. Electronics, 2021, 10, 64. DOI: https://doi.org/10.3390/electronics10010064.

[7] Ejaz W, ul Hasan N, Azam M A, et al. Improved local spectrum sensing for cognitive radio networks. EURASIP Journal on Advances in Signal Processing 2012, 2012, 242. DOI: https: //doi.org/10.1186/1687-6180-2012-242.

[8] Adardour H E, Meliani M, Hachemi M H. Improved local spectrum sensing in cluttered environment using a simple recursive estimator. Computers & Electrical Engineering 2017, 61, 208-222. DOI: https://doi.org/10.1016/j.compeleceng.2016.11.037.

[9] Quan Z, Zhang W, Shellhammer S J, et al. Optimal spectral feature detection for spectrum sensing at very low SNR. IEEE Transactions on Communications 2011, 59, 201-212. DOI: https://doi.org/10.1109/TCOMM.2010.112310.090306.

[10] Zhang B, Wu J, Su M, et al. An efffcient cooperative spectrum sensing for cognitive wireless sensor networks. IEEE Access, 2023, 11, 132544-132556. DOI: https://doi.org/10.1109/ACCESS.2023.3336654.

[11] Besson O. Impact of covariance mismatched training samples on constant false alarm rate detectors. IEEE Transactions on Signal Processing, 2021, 69, 755-765. DOI: https://doi.org/10.1109/ TSP.2021.3050567.

[12] Diskin T, Beer Y, Okun U, et al. CFARnet: deep learning for target detection with constant false alarm rate. SIGNAL PROCESSING, 2024, 223, 109543. DOI: https://doi.org/10.1016/j. sigpro.2024.109543.

[13] Li K, Zhang P, Yang Z. Semiparametric constant false alarm rate method for radar and sonar images. Electronics Letters, 2024, 60, e13146. DOI: https://doi.org/10.1049/ell2.13146.

[14] Zhong C, Wu C, Li X, et al. A novel frequency hopping prediction model based on TCN-GRU. IEICE Transactions on Fundamentals, 2024, E107-A, 1577-1581. DOI: https: //doi.org/10.1587/transfun.2023EAL2095.

[15] Zhou Z, Huang L, Christensen M G, et al. Robust spectral analysis of multi-channel sinusoidal signals in impulsive noise environments. IEEE Transactions on Signal Processing, 2022, 70, 919-935. DOI: https://doi.org/10.1109/TSP.2021.3101989.

[16] Ravve I, Koren Z. Analytical hilbert-transform attributes of ricker and gabor wavelets. IEEE Transactions on Geoscience and Remote Sensing, 2023, 61, 1-16. DOI: https://doi.org/10.1109/TGRS.20 40723.3309248.